

Identification and characterization of sorbed lutetium species on 2-line ferrihydrite by sorption data modeling, TRLFS and EXAFS

By K. Dardenne*, T. Schäfer, M. A. Denecke, J. Rothe and J. I. Kim

Forschungszentrum Karlsruhe, INE, P.O. Box 3640, D-76 021 Karlsruhe, Germany

(Received January 9, 2001; accepted January 11, 2001)

Lutetium / Sorption / EXAFS / Hydrous ferric oxide / Ferrihydrite / Sorption modeling

Summary. The Lu(III) sorbed species onto synthetic hydrous ferric oxide (HFO), commonly called ferrihydrite, has been identified. Characterization of the synthetic 2-line HFO shows that its synthesis is reproducible. Potentiometric titration of freshly synthesized HFO, modeled using the constant capacity model ($\kappa_1 = 0.5 \text{ F/m}^2$) in the FITEQL code, yields a specific surface area S_a of $360 \pm 35 \text{ m}^2/\text{g}$ (N_2 -BET), a site density N_d of 2.86 sites/nm^2 (concentration of hydroxyl groups, $N_s = 1.71 \times 10^{-3} \text{ mol sites/g HFO}$), and acidity constants $\text{p}K_{a1}^{\text{int}} = 6.37$ and $\text{p}K_{a2}^{\text{int}} = 9.25$.

Evaluation of chemical sorption data reveals the presence of two different Lu surface sorbed species, dependent on pH; a monodentate species forms at low pH and a polydentate species at $\text{pH} > 5$. Satisfactory fits to the sorption data are obtained using a combination of monodentate and bidentate surface species. The combination of species is chosen, based on extended X-ray absorption fine structure (EXAFS) results. The sorption constants obtained from these fits are $\text{p}K_s = -1.89(\pm 0.1)$ and $\text{p}K_s = -1.69(\pm 0.1)$ for the monodentate species $\equiv \text{FeOLu}(\text{H}_2\text{O})_5^{2+}$ for fits to the pH edge and to the isotherm at pH 5.9, respectively. A value of $\text{p}K_s = 3.69(\pm 0.01)$ is found for the bidentate species $\equiv \text{Fe}(\text{O})_2\text{Lu}(\text{H}_2\text{O})_5^+$ for both fits. EXAFS analysis of sorption samples prepared at $4.5 < \text{pH} < 8$ shows that Lu is surrounded by a single first shell of 7 ± 1 oxygen atoms, at a distance of $(2.30 \pm 0.01) \text{ \AA}$ in all samples. A second coordination shell of Fe neighboring atoms at a distance of $(3.38 \pm 0.01) \text{ \AA}$ is observed for sorption samples $\text{pH} \geq 5.5$. This distance is associated with the formation of a bidentate complex with bonding via edge sharing to iron octahedra. The samples prepared at $\text{pH} < 5.1$ show no Fe shell, as expected for monodentate coordination. No evidence for surface precipitation and no noticeable difference between wet paste and dried powder samples is found.

1. Introduction

Knowledge of the interaction of actinide cations with mineral surfaces is prerequisite to long-term performance assessment of nuclear repositories. Sorption models and corresponding equilibrium constants describing the actinide-mineral interaction are obtained from modeling of sorption data, i.e., the measured amount of actinide cations sorbed

onto a mineral surface as a function of pH, ionic strength, and actinide concentration. These models and the determined constants describing determinant aqueous/mineral-interface processes and mechanisms are used in predictive transport models for the long-term behavior of radionuclides. A mechanistic understanding of the processes involved, e.g., identification of the actinide species formed on the mineral surface, is important in modeling sorption data because the numerical equilibrium constant values extracted from the data are dependent upon the surface complexation reactions postulated. The reactants and reaction products assumed to participate in the sorption processes, i.e., the mineral sorption sites, actinide cation speciation, the sorbed surface species and their stoichiometries, influence the overall constants obtained in the modeling.

We have studied the surface sorption reaction of Lu(III) with low crystalline, metastable 2-line ferrihydrite, synonymously described in the literature [1] as hydrous ferric oxide (HFO). Lu is chosen as a homologue for the trivalent actinides. The equilibrium constants for the surface complexation reaction obtained from modeling sorption data are based on spectroscopic identification of the Lu sorbed species formed on the surface and experimental characterization of the HFO sorbent. Time resolved laser fluorescence spectroscopy (TRLFS) is not applicable for Lu(III) due to its full $4f$ shell. Therefore a TRLFS study is done using Eu and comparative studies of Eu and Lu sorption (pH edge and isotherms) are performed in parallel. Both lanthanides exhibit a similar HFO sorption behavior allowing transfer of Eu results to Lu. Lu is used for EXAFS studies instead of Eu because of the spectral interference of Eu L edges with the Fe K edge.

2. Materials and methods

2.1 2-line ferrihydrite (2L-HFO)

2.1.1 Preparation

Dispersion of HFO was freshly prepared according to Schwertmann and Cornell [2]. All chemicals were of analytical grade. The product was washed five times with Milli-Q water and separated after each washing by centrifugation. The concentrated suspension was dialyzed by a 3.0–3.5 nm dialysis membrane in a Milli-Q water bath for three days in

*Author for correspondence (E-mail: dardenne@ine.fzk.de).

the dark. The bath water was periodically changed. The resulting HFO stock solution had an electrical conductivity not greater than ten-times that of Milli-Q water and a concentration of approximately 14 g/mol. As HFO is a metastable phase, experiments were performed within three weeks to avoid the presence of HFO transformation products (hematite, goethite). Reproducibility of 15 separate syntheses was established by comparing physicochemical characterization of a freeze-dried aliquot from each charge.

2.1.2 Characterization

The synthetic HFO products were characterized by powder X-ray diffraction (XRD), Fourier transform infrared spectroscopy (FTIR), and surface area determination. The XRD patterns of powder samples were recorded using a Seifert 3000TT diffractometer with $\text{Cu } K_{\alpha}$ radiation. The patterns of all 15 charges were comparable, showing only two broad diffraction peaks at d spacings of 0.26 nm (110) and 0.15 nm (300), as expected for 2-line HFO [3]. No traces of 6-line HFO, transformation products (hematite or goethite), or impurities were detected.

FTIR analysis on KBr pellets (1.5 wt. % HFO) using a Bruker IFS55 spectrometer confirmed the purity of the synthetic 2-line HFO. Only characteristic hydroxyl bands at 450 and 650 cm^{-1} (bulk OH deformations), $\sim 3440 \text{ cm}^{-1}$ (bulk OH stretch), and an adsorption band at 1620 cm^{-1} (molecular water) were observed.

Specific surface area, S_A , measurements were performed by the BET [4] method using N_2 adsorption (Quantachrome, Autosorb1) and the modified ethylene-glycol-monoethyl-ether (EGME) method of Carter *et al.* [5]. The latter method is a widely accepted procedure [6] to measure the total (external and internal) surface area, where the molecular area occupied by an EGME molecule is defined as 0.52 nm^2 . Pre-treatment of BET samples included a drying and gas removal procedure at 105 °C. The S_A determined by EGME adsorption was $675 \pm 56 \text{ m}^2\text{g}^{-1}$ (number of determinations, $N = 31$) and from BET N_2 -adsorption, $360 \pm 35 \text{ m}^2\text{g}^{-1}$ ($N = 7$). These results are comparable to published values: 590 m^2/g by EGME adsorption [7] and BET- $\text{N}_2(\text{g})$ values of 340 m^2/g [8] and 313 m^2/g [9]. The S_A values from both methods are smaller than the theoretically calculated value of 840 m^2/g [10], assuming 2 nm diameter ferrihydrite spheres with a 3.57 g/cm^3 density.

2.2 Potentiometric and sorption experiments

2.2.1 Experimental procedure

Potentiometric titration experiments were performed to determine acidity constants and total concentration of the surface hydroxyl groups. An aqueous suspension of 1 g/L 2-line HFO was titrated with CO_2 -free HClO_4 or NaOH, over a pH range 4–10, at three different ionic strengths (0.1, 0.01, 0.001 mol/L NaClO_4), under inert gas atmosphere (Ar). The pH was measured using a Ross type standard combination electrode. During each titration, a maximum of ten to fifteen minutes between each incremental addition of base or acid were allowed for pH to equilibrate. This was to ensure that only ionization of surface hydroxyl groups

contributed to the determination of the surface acidity constants [11].

Lu(III) sorption batch experiments were performed on a 4.8 g/L aqueous suspension of HFO in 20 mL total volume, containing 10^{-3} mol/L Lu(III), at constant ionic strength (0.1 mol/L NaClO_4), and under inert gas atmosphere. Polypropylene or polyethylene vessels and storage containers were used for all sorption experiments. Lutetium was added from an acidic stock solution and 0.1 mol/L NaOH or HClO_4 used for pH adjustment. The pH was held constant at the desired value using a 10^{-3} mol/L 2-(N-morpholino)ethanesulfonic acid (MES) buffer in the pH range 5–6 and β -(4-pyridil)ethanesulfonic acid (PES) near pH 4. A maximum surface coverage of 12% to 24% was expected under these experimental conditions (2.1×10^{-4} mol Lu per g HFO), assuming a mono- or bidentate complexation. The samples were agitated regularly over three days. Lu and Fe concentrations of the supernatant solution following 35 min ultra-centrifugation at 450 000 g (XL90 Ultracentrifuge, Beckman) were determined by ICP-AES and ICP-MS (Perkin-Elmer PLASMA 400 & ELAN 6000). Fe concentrations were determined to avoid erroneously high Lu supernatant concentrations due to an possibly presence of HFO colloids. A portion of the separated solid phase, rinsed with Milli-Q water, was freeze-dried or dried 12 hours at 45 °C under aerobic conditions for spectroscopic investigations.

2.2.2 Fitting procedure

Surface acidity constants and Lu complexation constants were obtained by fitting the experimental pH titration and sorption data to surface complexation models (SCM) using the FITEQL 3.2 code [12]. The constant capacitance model (CCM) and diffuse double layer model (DDLM) were used for the titration data. The main indicator of the goodness of fit is the overall variance, V_y , which is the weighted sum of squares of residuals divided by the degree of freedom (SOS/DF). The weighting factor is the experimental error estimate calculated from the given experimental error so that the numerical value of V_y depends on experimental error estimates. A reasonably good fit is generally indicated by V_y values between 0.1 and 20 [12].

The error estimates used to fit the titration data are 7% for the relative error for pH, corresponding to an absolute error of 0.03 pH unit, and a relative error of 1% for the total proton concentration, corresponding to an absolute error of 10^{-6} mol/L. Fits to the pH-edge sorption data were performed using 4.6% (0.02 pH unit) as a relative error for pH and 10^{-5} mol/L as the absolute error for the sorbed species concentration. The isotherm sorption data was fitted using 9.2% (0.04 pH unit) as a relative error for pH. Relative errors of 1.5% and 3% were used for the total Lu concentration and the concentration of Lu remaining in solution.

2.3 Spectroscopic investigations

Time-resolved laser fluorescence spectroscopic (TRLFS) lifetime measurement of Eu(III) (${}^5D_0 \rightarrow {}^7F_i$) was used to determine the number of water molecules coordinated to Eu sorbed onto HFO. Eu was used as Lu does not fluoresce.

A dye laser (Exalite 398), pumped by a pulsed Nd:YAG laser (Continuum, Powerlite 9030, ND 6000) with a pulse energy of 3 mJ, was used. TRLS study was performed on KBr pellets containing Eu(III) sorbed onto HFO at pH 5.7 (1.1 wt. % HFO, 4.9×10^{-4} mol Eu/g HFO, maximal surface site coverage 28%). The Eu sorption onto HFO was achieved by the same procedure as described for Lu above. An excitation wavelength of 396.5 nm was used to promote the Eu^{3+} ions from the ground state 7F_x into the 5L_7 state, which decayed to the emitting 5D_0 level through non-radiative relaxation. Fluorescence emitted in the 540 nm to 740 nm range from the ${}^5D_0 \rightarrow {}^7F_x$ transition was detected by an optical multi-channel analyzer (polychromator Chromex 250) with a 300 lines/mm grating. The WINSPEC data acquisition software was used to register spectra. The time dependent emission was scanned by recording 51 spectra with increasing the delay time between laser pulse and camera gating from 1 μs to 1.5 ms by 30 μs interval.

EXAFS spectra were measured at the Hamburger Synchrotronstrahlungslabor (HASYLAB) positron storage ring DORIS, operating at 4.44 GeV with a maximal current of 150 mA, at beamline A1, as well as at the European Synchrotron Radiation Facility (ESRF), operating at 6 GeV with a maximal current of 200 mA, at the ROBL beamline. At HASYLAB, a double-bounce monochromator with a Si(111) channel-cut crystal was used. The monochromator was equipped with a piezo-driven feedback to stabilize the intensity of the incident X-ray beam [13]. The crystals were detuned to 50% of the incident intensity in order to obviate higher harmonic contamination of the beam. At the ROBL station, Si(111) crystals were used for the double-crystal monochromator, which was also stabilized with a feedback system. Higher harmonics were rejected by two Pt coated mirrors. All data were collected at ambient temperature in transmission mode, using ionization chambers filled with nitrogen gas.

A list of the samples investigated, their Lu loadings, experimentally measured Lu L_3 edge jumps, and the facility where their spectra were recorded are given in Table 1. EXAFS spectra were recorded at the Lu L_3 edge (9244 eV) for five Lu(III):HFO sorption samples prepared at varying pH and two reference samples, a 0.02 M aqueous Lu(III) solution and Lu_2O_3 . Powdered samples were measured dispersed in polyethylene (PE) powder and pressed into 13 mm \varnothing pellets. The wet paste sample was measured loaded

into a stoppered PE tube of 400 μL volume and a diameter of 5 mm. No drying occurred during data collection.

Sample spectra were energy calibrated using the first inflexion point in the K -edge spectrum of a zinc metal foil, defined as 9659 eV [14], which was recorded simultaneously. The EXAFS was extracted from the absorption spectrum by fitting μ_0 with a cubic spline function. The autobak program was also used to extract $\chi(k)$ from the absorption spectrum for comparison [15]. Data analysis was performed based on conventional methods [16] using the WinXAS97 software [17]. Theoretical backscattering amplitude and phase functions for fitting the experimental data were calculated with the multiple scattering code FEFF8 [18] either using single scattering Lu–O atom pairs or a 6 atom cluster with atomic positions calculated from the structural data reported for Lu_2O_3 [19].

3. Results and discussion

3.1 Titration modeling

The pH titration curves for three different ionic strengths are shown in Fig. 1. The curves are shifted along the ordinate to align the “pristine” point of zero charge at zero addition of base and acid [20]. The crossing point of these curves, called PZSE (point of zero salt effect), is found at a pH value of 7.8 and taken as the point of zero net proton charge, PZNPC. This value is comparable to 7.8–7.9 found by Charlet and Manceau [21] and Davies and Leckie [11] and to 7.9 to 8.2, with an average of 8.0, reported by Dzombak and Morel [1] using different methods including acid/base-titration, electrophoresis, and salt titration. This PZNPC is on the lower end of the range of published values. However, it cannot be interpreted as transformation of 2-line HFO to goethite, because such a conversion was not confirmed by IR spectroscopic and powder XRD results.

The point of zero net proton charge, PZNPC, is related to the intrinsic acidity constants, K_a^{int} , by the following expression:

$$\text{PZNPC} = 0.5 (\text{p}K_{a1}^{\text{int}} + \text{p}K_{a2}^{\text{int}}) .$$

The apparent acidity constant, K_a^{app} , can be calculated from K_a^{int} via the expression:

$$\text{p}K_a^{\text{app}} = K_a^{\text{int}} \exp(-\Delta ZF\Psi/RT) ,$$

Table 1. EXAFS samples, Lu(III) loadings, Lu L_3 edge jumps, and the facility where they were measured.

Samples	pH	Loading (mg Lu/g)	Lu in pellet (mg)	Measured edge jump	Facility
Lu(III):HFO	7.7	51	2.5 ± 0.1	0.11	HASYLAB
	6.1	93	^a	0.094	ESRF
	6.1	93	5.20 ± 0.01	0.43	ESRF
	5.5	61.4–64.5	3.3 ± 0.1	0.28	ESRF
	5.1	22–29	1.4 ± 0.2	0.092	HASYLAB
	4.6	0.1–9	0.3 ± 0.3	0.054	ESRF
Lu_2O_3	–	879	9.0	0.84	HASYLAB
Lu aquo species in 0.5 M HClO_4	–	–	–	0.22	HASYLAB

a: wet paste sample.

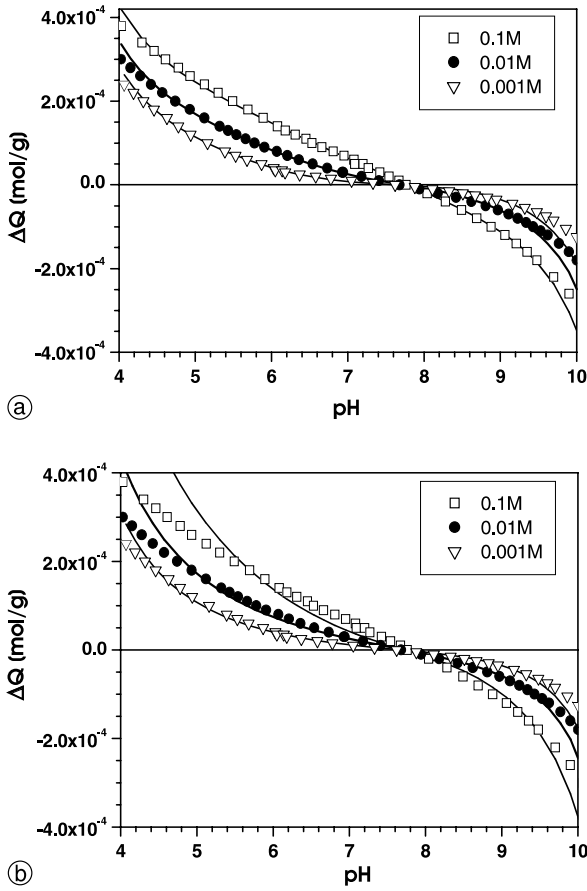


Fig. 1. Titration data (symbols) and resulting curves from FITEQL modeling (solid lines) using CCM top (a) and DDLM bottom (b).

Table 2. Results of fits to the titration data using CCM. DDLM results for a selected density of site (1.71×10^{-3} mol/g) are given for comparison.

I [mol/L]	pK_{a1}	pK_{a2}	PZC	WSOS/ DF	κ_1 [F/m ²]	N_d [sites/nm ²]	N_s [mol/g]	S_A [m ² /g]
0.1	6.56	9.06	7.81	2.10				
0.01	5.63	9.92	7.78	4.59	0.5	1.97 ^c	1.178×10^{-3c}	360
0.001	4.92	10.46	7.69	6.83				
0.1	6.37	9.25	7.81	2.08				
0.01	5.46	10.09	7.77	4.76	0.5	2.86	$1.710 \times 10^{-3*}$	360
0.001	4.75	10.62	7.69	6.94				
0.1	6.30	9.32	7.81	2.08				
0.01	5.39	10.15	7.77	4.82	0.5	3.28 ^c	1.960×10^{-3}	360
0.001	4.69	10.69	7.69	6.98				
0.1	6.56	9.06	7.81	2.10				
0.01	5.63	9.92	7.78	4.59	0.3	1.18 ^d	1.178×10^{-3}	600
0.001	4.92	10.46	7.69	6.83				
0.1	6.37	9.25	7.81	2.08				
0.01	5.46	10.09	7.77	4.76	0.3	1.72	$1.710 \times 10^{-3*}$	600
0.001	4.75	10.62	7.69	6.94				
0.1	6.30	9.32	7.81	2.08				
0.01	5.39	10.15	7.77	4.82	0.3	1.97 ^a	1.960×10^{-3}	600
0.001	4.69	10.69	7.69	6.97				
DDL M								
0.1	5.69	-9.79	7.742	53.88				
0.01	5.79	-9.71	7.751	12.36	-	2.86 ^e	1.710×10^{-3e}	360
0.001	6.14	-9.32	7.730	5.26				

a: values determined by Charlet & Manceau [21];

b: calculated from N_d and S_A and held constant during the fit procedure, excluding the two values marked*;

c: held constant during the fit and used to compared to the $S_A = 600$ m²/g results;

d: held constant during the fit and used to compared to the $S_A = 360$ m²/g results;

e: held constant during the fit and used to compared to the CCM results.

where ΔZ corresponds to the net charge change of the surface species and Ψ is the HFO surface potential in volt.

The isoelectrical point (IEP) was determined from electrophoretic mobility measurements for two ionic strengths 0.1 mol/L and 0.001 mol/L NaClO₄ and was found at a pH value of 8.7. This is in good agreement with the 8.5–8.8 values reported by Parks [22].

Surface acidity constants to describe the amphoteric character of the HFO surface hydroxyl groups



are calculated from the titration data using FITEQL 3.2. The constant capacitance, κ_1 , K_{a1}^{int} , K_{a2}^{int} , and the total concentration of surface hydroxyl groups, N_s , are the variable parameters for the three different ionic strengths investigated. Titration data was fitted in the manner described by Hayes *et al.* [23]), in which κ_1 and N_d (site density in sites/nm²) are held constant, while the values for K_{a1}^{int} and K_{a2}^{int} are varied, and the fit is repeated for various incremental values of κ_1 and N_d . The value for N_d is varied between 1 and 100 sites/nm² using literature values and κ_1 is varied between 0.2 and 1.2 F/m² in 0.1 increments. Due to the large difference in S_A determined by different methods, fits are performed for three S_A values: the BET-N₂ adsorption result (360 m²/g), the EGME adsorption result (675 m²/g), and the value recommended by Davis (600 m²g⁻¹) [1, 10, 11].

The best fit for all three ionic strengths is obtained using the CCM (see Fig. 1a, Table 2). With the DDLM (Fig. 1b,

Table 3. Experimentally determined PNZPC for hydrous ferric oxides(*) and low crystalline 2-line HFO and acidity constants at a ionic strength 0.1 M.

PZNPC	pK_{a1}	pK_{a2}	$N_s (10^{-3} \text{ mol sites/g HFO})$	Reference
7.85*	6.6	9.1	1.12	Farley <i>et al.</i> (1985) [28]
8.00	7.18	8.82	2.04	Dzombak & Morel (1990) [1]
7.83	6.93	8.72	2.04	Hansen <i>et al.</i> (1994) [20]
7.9*	5.1	10.7	9.86	Davis & Leckie (1978) [11]
7.8	6.37	9.25	1.71	This work

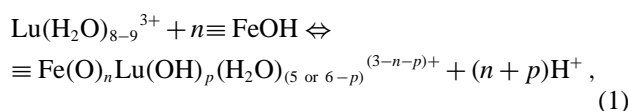
Table 2), only the lowest ionic strength in the pH-range 4.8 to 9.4 can be satisfactorily modeled. This fit, however, is not significantly better than that obtained using the CCM approach. The value used for κ_1 is found to be the most critical parameter. Best κ_1 values are 0.5 F/m^2 for $S_A = 360 \text{ m}^2/\text{g}$, 0.3 F/m^2 for $S_A = 600 \text{ m}^2/\text{g}$, and 0.25 F/m^2 for $S_A = 675 \text{ m}^2/\text{g}$. Using these values, fits of the titration data yield identical acidity constants for a given N_s , with comparable SOS/DF values for each S_A . We retain the surface area obtained by BET because it does not include micro pores, which might not be available for “fast” sorption processes. It is evident from the results in Table 2 that it is impossible to select the “true” acidity constants based on the SOS/DF variation obtained for the three best fits. Therefore the set of values obtained by optimizing N_s is selected. The following acidity constants are found: $pK_{a1}^{\text{int}} = 6.37$ and $pK_{a2}^{\text{int}} = 9.25$, $N_s = 1.71 \times 10^{-3} \text{ mol/g}$ with $N_d = 2.86 \text{ sites/nm}^2$ for $S_A = 360 \text{ m}^2/\text{g}$ in $0.1 \text{ mol/L NaClO}_4$. These values are used for modeling the Lu sorption described below.

A range of acidity constants, derived from experimental data for HFO, has been reported in the literature and is given Table 3. In the present investigation, the reproducibility of each solution of 2-line HFO is painstakingly validated. Only freshly precipitated products are used for potentiometric and Lu sorption investigations.

Surface speciation calculated with these constants shows that more than 80% of the proton exchangeable groups are in the form $\equiv \text{FeOH}$; the relative $\equiv \text{FeOH}$ concentration variation is less than 6% in the pH range 4–10.

3.2 pH-edge and isotherm sorption modeling

The Lu pH-edge sorption curve is shown in Fig. 2. The sorption edge is graphically found to be at $\text{pH} = 5.2$. The maximal sorption is attained at $\text{pH} 6$ under the conditions investigated. The sorption equilibrium reaction can be written as follows:



where $\equiv \text{FeOH}$ describes one surface HFO hydroxyl group and $\equiv \text{Fe}(\text{O})_n$ defines the number of hydroxyl groups reacting with a Lu^{3+} cation. Lutetium bound to hydroxyl groups connected to the same iron atom on the HFO surface (edge sharing polyhedron) or to hydroxyl groups connected to different, adjacent iron atoms (corner sharing iron polyhedron) are not distinguished in this description.

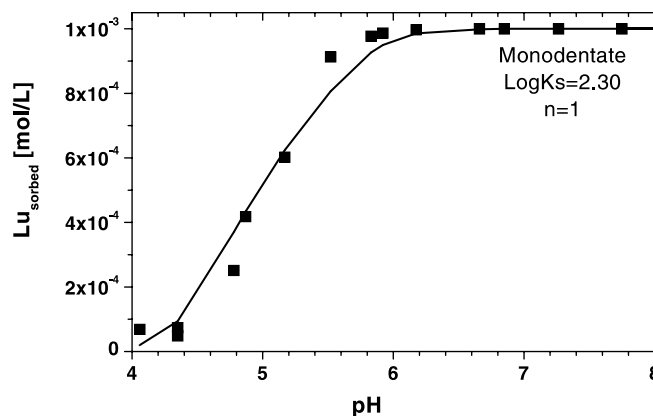


Fig. 2. Experimental pH edge (symbols) and theoretical fit using a monodentate species (WSOS/DF: 11.9) and CCM.

The rearrangement of the expression for the sorption constant, K_s , defined by Eq. (1) yields:

$$\log \frac{[\text{Lu}_{\text{sorbed}}]}{[\text{Lu}^{3+}]_{\text{aq}}} = (n+p)\text{pH} + \log K_s + n \log [\equiv \text{FeOH}]_{\text{free}},$$

where $[\text{Lu}_{\text{sorbed}}]$ represents the concentration of surface sorbed species, $\text{Fe}(\text{O})_n \text{Lu}(\text{OH})_p (\text{H}_2\text{O})_{(5-p)}^{(3-n-p)+}$, and $[\text{Lu}^{3+}]_{\text{aq}}$ the concentration of aquo species in solution, $\text{Lu}(\text{H}_2\text{O})_8^{3+}$. The relative concentration variation of free surface hydroxyl groups is near 2, 5, and 10%, for a monodentate (**M**; $n = 1$), bidentate (**B**; $n = 2$), or tridentate (**T**; $n = 3$) sorbed species, respectively. As a first approximation, this concentration variation is small and can be neglected. Then a linear relationship exists between pH and

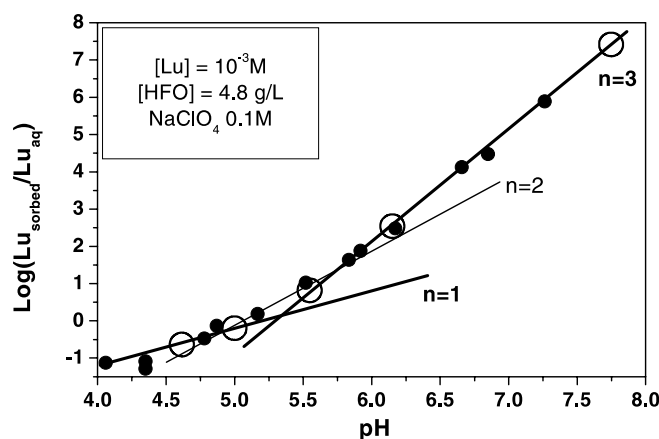


Fig. 3. Log-log plot of the pH edge. Experimental points are small filled circles; EXAFS samples are indicated as large open circles. Differentiation into three regions of different slopes is based on CCM modeling and results from EXAFS experiment described in Sect. 3.4.

log $\frac{[Lu_{\text{sorbed}}]}{[Lu^{3+}]_{\text{aq}}}$. The corresponding so-called “log-log” plot is shown in Fig. 3. Each slope gives the total number of protons exchanged in the sorption process, $(n + p)$. At least two different regions can be distinguished in Fig. 3: one region at $\text{pH} < 5.3$ with a slope 1 and one at $\text{pH} > 5.3$ with a slope in the range 2.65–2.75, or near 3. The graphical approximation indicates that at least two types of sorbed surface species are formed. The sorbed species at $\text{pH} < 5.3$ should satisfy the relation $(n + p) = 1$ and at $\text{pH} > 5.3$ $(n + p) \sim 3$. The value of n gives the dentate character of the sorbed species and can vary from 1 to 3. The value p defines the degree of hydrolysis and varies from 0 to 2. Refinement to the graphical approach by including the variation of the surface hydroxyl group concentration does not noticeably change the slope of the “corrected” log–log plot. Differentiation of the log–log plot into three regions of slopes 1, 2, and 3 indicated in Fig. 3 is based on subsequent modeling and the results from EXAFS experiment described in Sect. 3.4. If the slope in the log–log plot is determined within the pH range limited to 4.7–6.2, i.e., above the pH where a single monodentate species forms and below the pH where hydrolysis occurs, then a value of about 2 is obtained, the value expected for the formation of a bidentate species without hydrolysis.

The Lu(III):HFO sorption data are also modeled using the FITEQL 3.2 code and various $\text{Fe}(\text{O})_n\text{Lu}(\text{OH})_p \cdot (\text{H}_2\text{O})_{(5-p)}^{(3-n-p)+}$ surface species. The quality of the fit obtained using a single sorbed species is poor. An example for a single, monodentate surface species is shown in Fig. 2. The best fit results are achieved when including two species in the model, one with $(n + p) = 1$ and the other with $(n + p) = 3$. The combination $(n + p) = 1$ and $(n + p) = 2$ species also leads to good quality fit results. Depending on which combination is used, monodentate $(n + p) = 1$ and a $(n + p) = 2$ species or monodentate $(n + p) = 1$ and a $(n + p) = 3$ species, two general speciation curves are obtained as shown in Fig. 4. The $\text{p}K_s$ values obtained for the combined species fits are listed in Table 4.

Fig. 5 compares the best fit results for a single species fit with that obtained using a fit model of a combination

Table 4. Sorption constants ($\text{p}K_s$) obtained with CCM modeling of Lu(III):HFO pH edge data for the surface species $\text{Fe}(\text{O})_n\text{Lu}(\text{OH})_p \cdot (\text{H}_2\text{O})_{(5-p)}^{(3-n-p)+}$ using $S_A = 360 \text{ m}^2/\text{g}$, $N_d = 2.86$. 1:2 indicates using a model of combined monodentate (**M**; $n = 1$) and bidentate (**B**; $n = 2$) species; 1:3 a combination of **M** and tridentate (**T**; $n = 3$).

$n + p$	M	MOH	$\text{M}(\text{OH})_2$	B	BOH	T	WSOS/DF
1	-2.30						11.9
2		5.52		3.31			7.8
			12.80				7.1
3					10.55		12.9
						8.23	11.1
1:2	-1.89			3.69			8.2
	-1.91	5.91					4.3
1:3	-2.03		13.95				4.1
	-2.03				11.75		3.7
	-2.02					9.52	3.8

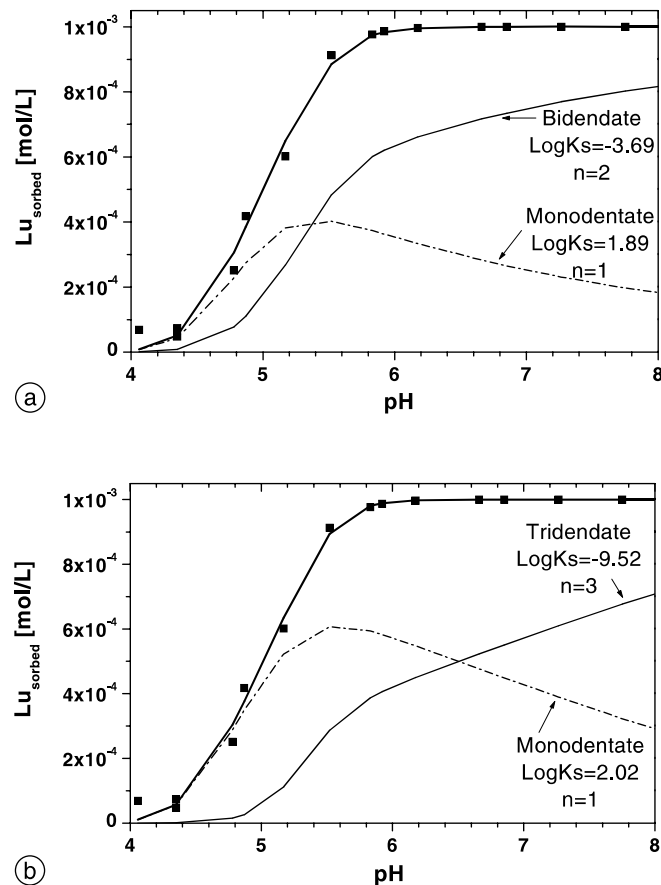


Fig. 4. (a): Speciation curves calculated from modeling results (WSOS/DF = 4.1–4.3) for combination of monodentate $n = 1$ and $n = 2$ species. (b): corresponding curves from modeling results (WSOS/DF = 3.7–3.8) obtained for a combination of monodentate $n = 1$ and $n = 3$ species.

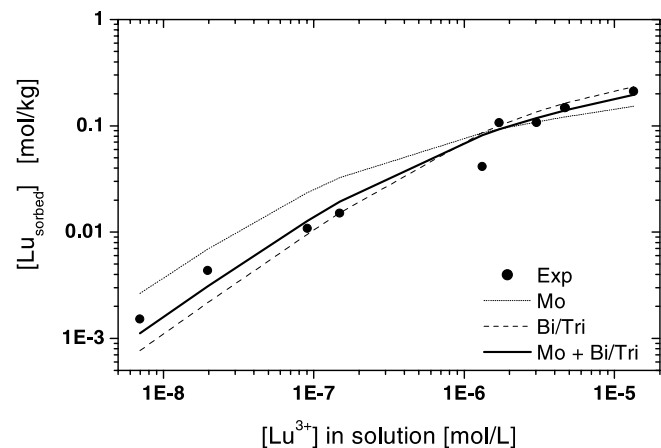


Fig. 5. CCM fits to the sorption isotherm at pH 5.9 from results listed in Table 5. Mo is using $(n + p) = 1$ species. Bi/Tri are actually two results for $n = 2$ and another for $n = 3$. Mo + Bi/Tri is also two results for 1:2 and 1:3 species combination in Table 5. In both cases, the two results yield curves which are identical to within the line width shown.

of species. Modeling the isotherm sorption measured at pH 5.9 yields the same results for $\text{p}K_s$ (Table 5) as found for modeling the pH edge. Similar to the pH-edge results, a satisfactory fit is only possible for a combination of two surface species. The relative concentrations of the two Lu sorbed species found for the isotherm at pH 5.9 are in good agree-

Table 5. Sorption constants (pK_s) obtained with CCM modeling of the Lu(III):HFO pH isotherm at pH 5.9 for the surface species $\text{Fe}(\text{O})_n\text{Lu}(\text{OH})_p(\text{H}_2\text{O})_{(5-p)}^{(3-n-p)+}$ using $S_a = 360 \text{ m}^2/\text{g}$, $N_d = 2.86$. 1:2 indicates using a model of combined monodentate (**M**; $n = 1$) and bidentate (**B**; $n = 2$) species; 1:3 a combination of **M** and tridentate (**T**; $n = 3$).

$n + p$	M	B	BOH	T	WSOS/DF
1	-2.30				19.3
2		3.44			4.98
3			10.86		9.52
				8.63	4.34
1:2	-1.69	3.69			3.1
1:3	-1.90		11.8		2.7
	-1.89			9.57	2.7

ment to those obtained from analysis of the pH-edge. The relative concentrations calculated are either $\sim 33\%$ **M** and 64% **B** or $\sim 57\%$ **M** and 42% **T**, depending on the polydentate species which is assumed.

No final conclusion can be drawn concerning the nature of the sorbed species based only on modeling of the sorption data. One may conclude that two different Lu sorbed species appear to form on the HFO surface in the pH and concentration range studied. One of these species is a monodentate species; further information is needed in order to identify the second, polydentate species.

3.3 TRLFS results

The variation of the lifetime with the number of coordinated water molecules is explained by the de-excitation through vibronic coupling process. In the case of lanthanides, it has been shown that the rate of deexcitation via a vibronic coupling between OH oscillators and Ln(III) ions can be assumed to be “directly proportional to the number of OH oscillators in the first coordination sphere” [24].

As mentioned in Sect. 1, laser fluorescence measurements can not be performed on Lu due to its $4f$ full shell. Therefore, Eu, which shows a similar sorption behavior is chosen for TRLFS experiments. The Eu sorption sample is obtained by the same experimental procedure used for Lu. The TRLFS studies are performed on KBr pellets containing Eu(III) sorbed onto HFO at pH 5.7 (1.1 wt. % HFO, 4.9×10^{-4} mol Eu/g HFO, maximal surface site coverage of 28%). The Eu sorption species is characterized by a lifetime of 205 μs . An increase of the lifetime over the lifetime of the aquo species (110 μs) indicates that the number of water molecules in the first Eu(III) coordination sphere is reduced from nine (or ten) in the aquo species [24] to five water molecules (including OH) in this sorption sample.

3.4 EXAFS results

In order to identify the two Lu surface sorbed species, EXAFS experiments are performed on Lu(III):HFO sorption samples. Samples are specifically selected distributed across regions in the log-log representation of the pH edge (Fig. 3): pH 4.6, 5.1, 5.5, 6.1, and 7.7. Lutetium L_3 edge

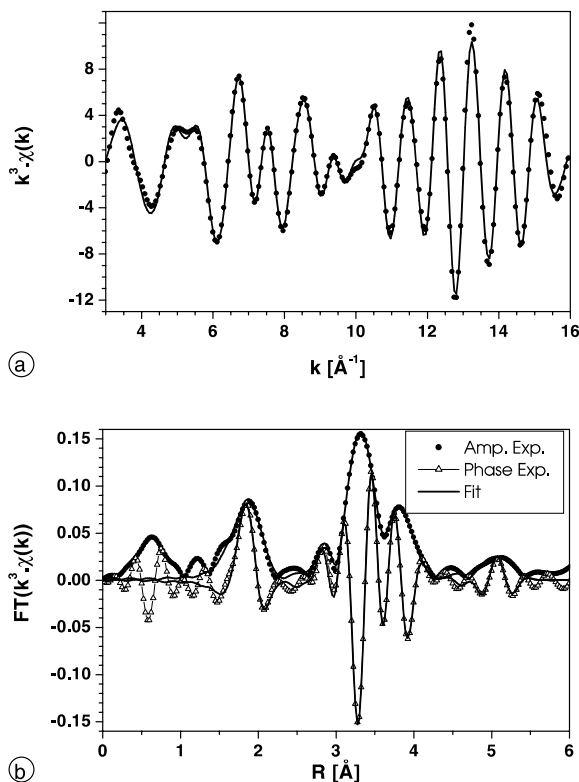


Fig. 6. (a) k^3 -weighted Lu L_3 edge EXAFS for Lu_2O_3 (line) and best fit results (dots) using phase and backscattering functions obtained from single scattering phase and amplitude functions. (b) Corresponding Fourier transform (Bessel window, k range = $3.0\text{--}16.0 \text{ \AA}^{-1}$). The fit in this curve is depicted as a line.

EXAFS spectra of the reference samples are analyzed in order to test the theoretical backscattering amplitude and phase functions used in the data analysis. Fig. 6 shows the k^3 -weighted EXAFS spectrum for Lu_2O_3 , its corresponding Fourier transform (FT) and the theoretical functions obtained from fits of the experimental data to the EXAFS equation using the functions obtained from the atom cluster FEFF8 calculation. Fits are performed to both

Table 6. Structural parameters obtained from fits to Lu_2O_3 EXAFS in both R -space and k -space (*italics*) and shown in Fig. 5. The amplitude reduction factor, S_0^2 , was held constant at 1. The shift in ionization energy, ΔE_0 , was held constant at 7.46 eV for fits in R -space and at 7.50 eV for those in k -space. Average bond lengths and coordination numbers calculated from XRD structure determination (JCPDS-ICDD 43-1021, Saiki, 1985) are given in parentheses.

Bond	R [\AA]	N	$\sigma_2 \cdot 10^{-3}$ [\AA^2]
Lu–O	2.22	6.5	6.8
	2.22	6.0	6.0
	(2.246)	(6)	
Lu–Lu	3.45	7.1	4.9
	3.45	6.4	4.5
	(3.453)	(6)	
Lu–Lu	3.93	5.1	4.6
	3.93	5.2	4.8
	(3.933)	(6)	
Lu–Lu	5.19	8.1	8.2
	5.19	7.9	8.3
	(5.223)	(6)	

the EXAFS oscillations and to the FT spectra (i.e., fits in k -space and R -space). The coordination number, N , interatomic distance, R , and EXAFS Debye–Waller factor, σ^2 , obtained from the fits are listed in Table 6. The results are in good agreement with the XRD structure determination [19, JCPDS-ICDD 43-1021].

The fit to the Lu(III) aquo species spectrum, used as a reference sample, using FEFF8 scattering functions from the cluster calculation gives 8 oxygen neighbors at a distance of 2.31 Å with $\sigma^2 = 0.0058 \text{ \AA}^2$. The smaller σ^2 value for the Lu–O sphere in the aquo species compared to Lu_2O_3 reflects the smaller distribution of bond lengths in the solution species. In the Lu_2O_3 structure, there are two crystallographic Lu sites with a distribution of bond lengths from 2.18 to 2.28 Å. This leads to a larger σ^2 value of 0.0068 \AA^2 for the Lu–O shell. Fits to the aquo species EXAFS using single scattering FEFF8 files give 9 oxygen neighbors at a 2.31 Å distance with $\sigma^2 = 0.0078 \text{ \AA}^2$. The fits using FEFF8 functions obtained from single scattering and cluster calculations yield the same results to within the range of error generally associated with an EXAFS analysis, i.e. $\pm 10\%$ for the coordination number and $\pm 0.02 \text{ \AA}$ for the interatomic distance. Thus the backscattering amplitudes and phase functions obtained from the single scattering calculations are used to analyze the Lu–O shell in the sorption sample spectra. Single scattering amplitude and phase functions for the Lu–Fe scattering pair are also used in fits to those sorption samples exhibiting a further distant Fe coordination shell.

The k^3 -weighted Lu L_3 edge EXAFS spectra for air-dried Lu(III): HFO sorption samples and their corresponding FT's are shown Fig. 7. From visual comparison of the spectra, it is evident that the sample prepared at pH 4.6 shows a larger oscillatory amplitude than the other samples. Furthermore, this sample shows no evidence for further distant coordination shells, whereas the other four samples all exhibit a FT peak at $\sim 3.1 \text{ \AA}$. Although the intensity of this peak is small, its presence corresponds to the perturbation of the main oscillation frequency in the EXAFS spectra at around 7 \AA^{-1} .

The EXAFS equation is fit to the spectra in both R - and k -space. Fits are repeated after applying different EXAFS extraction procedures. Fits of the FT data for a single Lu–O shell are initially performed within a 1.35–2.50 Å R -space window. Results for the Lu–O shell are introduced as starting parameters for fits in the 1.35–3.60 Å range using two

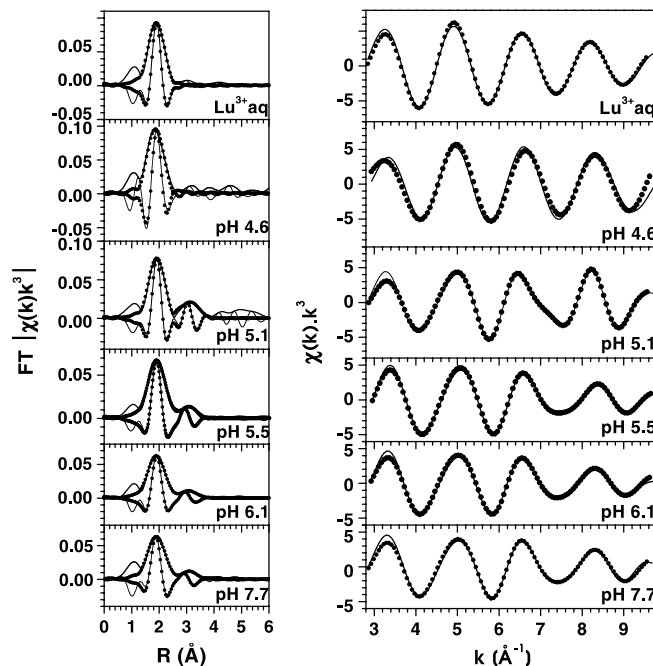


Fig. 7. Right: k^3 -weighted Lu L_3 edge filtered EXAFS (two first shells) and best fit results. Left: Fourier transform of the experimental EXAFS (Bessel window, k range = 2.6–9.9 \AA^{-1}). Theoretical curves are depicted as dots and experimental as continuous lines.

shells, both Lu–O and Lu–Fe shells. Fits in k -space are done on Fourier filtered FT spectra using a single oxygen coordination shell for the pH 4.6 sample and a model of one Lu–O and one Lu–Fe coordination shell for the other sorption sample spectra. These fits result in slightly greater σ^2 values and ~ 0.5 larger N than the fits in R -space. ΔE_0 is allowed to vary in the fits because not all spectra are recorded during the same experimental run or at the same facility. Setting $\Delta E_0 = 6.5 \text{ eV}$ constant for the three samples measured at ROBL during the same run yields the same results within the experimental error range.

Average values of all results obtained from fits in R - and k -space and for different EXAFS extraction procedures are summarized in Table 7. The standard deviations given in Table 7 are the statistic standard deviations of the numerous fit results. A comparison of structural parameters for the sorption samples reveals that the Lu–O distance is 2.30 Å for all samples; no splitting of the Lu–O coordination sphere upon binding to the HFO surface is observed. Within the experimental error, N is invariant for all

Table 7. Average structural parameters N, R and their statistical error obtained from fits described in the text. S_0^2 was held constant at 1.

Sample	pH	N	Lu–O			N	Lu–Fe		
			R [Å]	σ^2 10^{-3} [Å ²]	ΔE_0 [eV]		R [Å]	σ^2 10^{-3} [Å ²]	ΔE_0 [eV]
Lu(III):HFO	4.6	6.2 ± 0.8	2.28	2.5 ± 0.5	3.9	—	—	—	—
Lu(III):HFO	5.1	6.5 ± 0.5	2.31	6.1 ± 0.5	5.6	1.7 ± 0.3	3.48	6.3 ± 1.7	4.6
Lu(III):HFO	5.5	7.7 ± 1.0	2.30	10.3 ± 1.3	7.0	2.7 ± 0.8	3.38	15 ± 3	3.9
Lu(III):HFO	6.1	7.6 ± 0.6	2.30	10.5 ± 1.0	6.5	3.2 ± 0.8	3.38	21.5 ± 3	3.4
Lu(III):HFO ^a	6.1	7.3 ± 0.4	2.30	7.7 ± 0.6	6.5 ^b	2.7 ± 0.4	3.38	17 ± 2	3.4 ^b
Lu(III):HFO	7.7	7.0 ± 0.5	2.30	9.2 ± 0.7	6.1	3.3 ± 0.3	3.38	20.5 ± 0.4	3.2
Lu(III) aquo		9.1 ± 0.3	2.31	7.8 ± 0.5	4.9				

a: wet paste sample;

b: held constant at the value obtained for the dried sample, pH 6.1.

Lu(III):HFO sorption, 6–8. The only change in the metrical parameters as a function of sample preparation pH is in σ^2 . The larger Lu–O EXAFS intensity observed for the sample prepared at pH 4.6 is due to a smaller σ^2 (0.0025 \AA^2), which is even smaller than that observed for the Lu aquo species (0.0078 \AA^2), and not a larger N . The proximity of the HFO surface has an effect of lowering the mean square displacement of oxygen atoms coordinated to Lu(III). The oxygen atoms coordinating Lu belong mostly to water molecules. This means that the proximity of the HFO surface lends rigidity and/or increased order to the coordinating aquo sphere.

As expected from the TRLFS results, N is reduced by two to three for the sorption samples as compared to the aquo species. From TRLFS it is known that, following the sorption process at pH 5.7, five water molecules remain coordinated to the metal cation. Combining this information with the EXAFS results ($N \sim 7$), indicates that two next neighbor oxygen atoms belong to the HFO surface, i.e., a bidentate surface complex is apparently formed.

In order to interpret the results for the Lu–Fe parameters listed in Table 7, a discussion of the possible Lu–Fe interactions is required. Possible binding sites for Lu(III) onto a FeO_6 -octahedron located on the HFO surface are depicted in Fig. 8: a monodentate species (**M**), two possible bidentate species (bidentate edge-sharing **B1** and bidentate geminal corner-sharing **B2**), and a tridentate species (**T**). A double-edge sharing tridentate species is not included in these considerations because it is considered not to be energetically favorable [25]. The expected Lu–Fe distances for the different binding modes are also indicated in Fig. 8. Relatively long distances in the 3.7–4.4 Å range, depending on binding angle ($\angle \text{Fe–O–Lu}$), are expected for **M**. Species **B2** is expected to have Lu–Fe distances near 4.1 Å; **T** near 3.2 Å.

T is bound to a FeO_6 -octahedron face and expected to have a shorter Lu–Fe distance, $\sim 2.9 \text{ \AA}$. These Lu–Fe distances are based on the proposed structure for HFO basic tetrameric unit composed of four planar $\text{Fe}(\text{O}, \text{OH})_6$ octahedra [3], the d spacings from the HFO XRD pattern, and the Lu–O bond length from our EXAFS analysis.

Returning to the interpretation of Lu(III):HFO EXAFS fit results, no Lu–Fe interaction is observed for the pH 4.6 sample. This corroborates sorption results, which indicate the formation of **M** species at this pH. Due to both the long length expected for this interaction and the dynamic atomic displacements possible for **M** binding, a Lu–Fe interaction is not expected in the EXAFS. The appearance of a second peak at $\sim 3.1 \text{ \AA}$ (uncorrected for phase shift) for pH 5.1 and above results from scattering on a heavy atom and is attributed to a Lu–Fe interaction. No reliable fit of the data using Lu–Lu phase and amplitude scattering function is possible. The lack of a Lu–Lu interaction excludes the presence of sorbed polynuclear surface species or significant surface precipitation. A minor fraction of poorly ordered Lu-precipitate might not be detected. The $\sim 3.1 \text{ \AA}$ peak indicates the formation of a species different from species **M**, present at pH 4.6. The species **B1**, **B2**, and **T** have shorter Lu–Fe distances than species **M**, as well as a more rigid structure so that a Lu–Fe interaction should be observed in the EXAFS. The mean Lu–Fe distance found in the fits, 3.38 \AA , is the same for all sorption samples above pH 5.1, i.e. in the region where the slope in the log–log plot is around 3. This 3.38 \AA distance is too short for a **M** or **B2** species and too long to be associated with a tridentate species **T**. This distance better matches that expected for **B1**. These iron oxide polyhedron edge sites are high affinity bonding sites in HFO [25, 26]. A value of one for N (Lu–Fe) is expected for species **B1** but values ranging

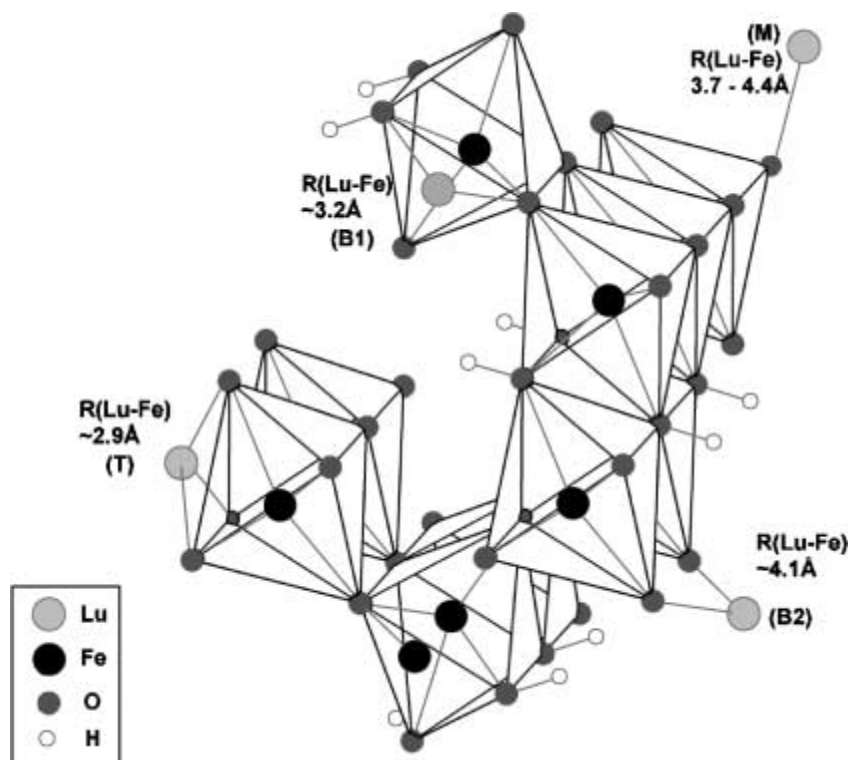


Fig. 8. Schematic, arbitrary structural representation of HFO surface sites available for Lu sorption and their calculated expected bond lengths (see text).

from 1.7 to 3.3 are obtained in the EXAFS analysis. This discrepancy may be due to the strong correlation between fit parameters N and σ^2 or to the Fe backscattering amplitude function used in the fit. We had no reference compound to test the amplitude function.

The σ^2 factor for the Lu–O shell increases with increasing pH. In addition, Lu–Fe shell exhibits a relatively large σ^2 factor. The Lu–O distance for a Lu–OH interaction should be different than the remaining Lu–O distances in the surface complex. Therefore, the introduction of an OH ligand into the Lu coordination sphere upon hydrolysis is expected to lead to an increase in the σ^2 factor of the Lu–O shell. The large Lu–Fe σ^2 values may indicate the presence of a distribution of Lu–Fe bond lengths. This might be expected for low crystalline HFO as sorbent, especially when hydrolysis occurs.

The pH 6.1 sorption sample is investigated both as a wet paste and a dried powder. However, no significant difference in their EXAFS spectra is observed. Fit results of the paste sample yield the same distances and comparable results for N , but a slightly smaller σ^2 value for both Lu–O and Lu–Fe coordination shells. Obviously, drying the sorption sample does not greatly alter the primary interaction of Lu(III) with the HFO surface. This is important to establish the relevance of the TRLFS hydration number, obtained for a dried sample.

4. Conclusions

Potentiometric titration of freshly synthesized HFO, modeled using the constant capacity model ($\kappa_1 = 0.5 \text{ F/m}^2$) with the FITEQL code, yields the following characteristics: a specific surface area of $360 \pm 35 \text{ m}^2/\text{g}$ (N_2 -BET), a site density N_d of 2.86 sites/ nm^2 ($N_s = 1.71 \times 10^{-3} \text{ mol sites/g HFO}$), and acidity constants $\text{p}K_{a1} = 6.37$ and $\text{p}K_{a2} = 9.25$. Chemical sorption studies shows that two different Lu species are sorbed onto HFO as a function of pH: a monodentate species forms at pH values < 5.1 and a polydentate species dominates at $\text{pH} > 5.1$.

The combination of modeling chemical sorption data and spectroscopic investigations, which probe the local structure of sorbed species, allows identification of the sorbed species. EXAFS results for Lu(III):HFO sorption samples prepared in the pH range 4.6 to 7.7 show that their EXAFS spectra exhibit a single first shell of 7 ± 1 oxygen atoms around Lu atoms at a distance of $(2.30 \pm 0.01) \text{ \AA}$. The coordination number of Lu sorbed onto HFO is lower than that of the aquo species (9 ± 1), but the Lu–O bond lengths are comparable, without evidence of any splitting of the first coordination shell into more than one distance. No evidence of surface precipitation is found. No noticeable difference is discernable between wet paste and dried powder samples.

At pH values below 5.1 the formation of the Lu sorption species takes place according to the reaction $\equiv \text{Fe}-\text{OH} + \text{Lu}^{3+}(\text{H}_2\text{O})_{8-9} \rightarrow \equiv \text{Fe}-\text{O}-\text{Lu}(\text{H}_2\text{O})_5^{2+} + \text{H}^+ + 3-4\text{H}_2\text{O}$. A second shell of neighboring Fe atoms at a distance near 3.4 \AA is found for the sorption samples prepared at pH values 5.1 and above. This Lu–Fe distance indicates that Lu forms a bidentate complex, with bonding via edge sharing with FeO_6 -octahedra on the HFO surface.

The sorption data are well fit using a combination of monodentate and bidentate species. The sorption constants of $\text{p}K_s = -1.89(\pm 0.1)$ and $\text{p}K_s = -1.69(\pm 0.1)$ for the monodentate species are found for fits to the pH edge and to the isotherm at pH 5.9, respectively. A value of $\text{p}K_s = 3.69(\pm 0.01)$ is obtained for the bidentate species $\equiv \text{Fe}(\text{O})_2\text{Lu}(\text{H}_2\text{O})_5^+$. The fact that the slope of the pH edge log–log plot is apparently greater than two, the value expected for the formation of the bidentate species, is interpreted as resulting from the hydrolyzed form of the bidentate complex. Above pH 6.5 the first hydrolysis $\text{Lu}(\text{OH})^{2+}$ species forms [27]. The EXAFS Debye-Waller factor for the sorption samples is observed to increase slightly with increasing pH. This is likely due to an increase in distribution of bond lengths in the Lu coordination sphere upon increasing the amount of hydrolyzed complexes.

Acknowledgment. We acknowledge the European Synchrotron Radiation Facility and the Hamburger Synchrotronstrahlungslabor (HASYLAB) for beamtime allotment and C. Hennig and T. Reich (ROBL, ESRF) and K. Attenkofer and E. Welter for their assistance.

References

- Dzombak, D. A., Morel, F. M. M.: *Surface complexation modeling – hydrous ferric oxide*. John Wiley & Sons, New York (1990).
- Schwertmann, U., Cornell, R. M.: *Iron Oxides in the Laboratory (Preparation and Characterization)*. VCH-Verlag, Weinheim (1991).
- Cornell, R. M., Schwertmann, U.: *The Iron Oxides – structure, properties, reactions, occurrence and uses*. VCH-Verlag, Weinheim (1996).
- Brunauer, S., Emmett, P. H., Teller, F.: Adsorption of gases in multimolecular layers. *J. Am. Chem. Soc.* **60**, 309 (1938).
- Carter, D. L., Heilman, M. D., Gonzales, C. L.: Ethyleneglycol monoethyl ether for determining surface area of silicate minerals. *Soil Sci.* **100**, 356 (1965).
- USDA.: Procedures for collecting soil samples and methods analysis for soil survey. U.S. Gov. Print. Office, Washington DC (1982).
- Pyman, M. A. F., Posner, A. M.: The surface areas of amorphous mixed oxides and their relation to potentiometric titration. *J. Colloid Interface Sci.* **66**, 85 (1978).
- Eggleton, R. A., Fitzpatrick, R.: New data and a revised structural model for ferrihydrite. *Clays Clay Min.* **36**, 111 (1988).
- Weidler, P. G.: Oberflächen synthetischer Eisenoxide. Dissertation, Techn. Universität München (1995).
- Davis, J. A.: Adsorption of trace metals and complexing ligands at the oxide/water interface. PhD, Stanford University, California (1977).
- Davis, J. A., Leckie, J. O.: Surface ionization and complexation at the oxide/water interface. II. Surface properties of Amorphous Iron Oxyhydroxide and Adsorption of Metal Ions. *J. Colloid Interface Sci.* **67**, 90 (1978).
- Herbelin, A., Westall, J.: FITEQL, A computer program for determination of chemical equilibrium constants from experimental data, Version 3.2. Oregon State University (1996).
- Krolzig, A., Materlik, G., Swars, M., Zegenhagen, J.: A feedback control system for synchrotron radiation double crystal instruments. *Nucl. Instr. Methods* **219**, 430 (1984).
- McMaster, W. H., Kerr Del Grande, N., Mallett, J. H., Hubbell, J. H.: Compilation of X-ray cross sections. Lawrence Livermore National Laboratory (1969).
- Newville, M., Livins, P., Yacoby, Y., Rehr, J. J., Stern, E. A.: *Phys. Rev. B* **47**, 14 126 (1993).
- Koningsberger, D. E., Prins, R.: *X-ray Absorption: Principles, Applications, Techniques for EXAFS, SEXAFS and XANES*. Wiley Interscience, New York (1988).

17. Ressler, T.: WinXAS: A New Software Package not only for the Analysis of Energy-Dispersive XAS Data. *J. Physique IV* **7**, 269 (1997).
18. Ankudinov, L. A., Ravel, B., Rehr, J. J., Conradson, S. D.: Real-space multiple scattering calculation and interpretation of X-ray-absorption near-edge structure. *Phys. Rev. B* **58**, 7565 (1998).
19. Saiki, A., *et al.*: *J. Ceram. Assoc. Jpn.* **93**, 649 (1985).
20. Hansen, H. C. B., Wetche, T. P., Raulung-Rasmussen, K., Borggaard, O. K.: Stability constants for silicate adsorbed to ferrihydrite. *Clay Minerals* **29**, 341 (1994).
21. Charlet, L., Manceau, A. A.: X-ray absorption spectroscopic study of the sorption of Cr(III) at the oxide/water interface. II. Adsorption, coprecipitation, and surface precipitation on hydrous ferric oxide. *J. Colloid Interface Sci.* **148**, 443 (1992).
22. Parks, G. A.: The isoelectric points of solid oxides, solid hydroxides, and aqueous hydroxo complex systems. *Chem. Rev.* **65**, 177 (1965).
23. Hayes, K. F., Redden, G., Wendell, E., Leckie, J. O.: Surface complexation models: an evaluation of model parameters estimation using FITEQL and oxide mineral titration data. *J. Colloid Interface Sci.* **142**, 448 (1991).
24. Horrocks, W. D. J., Sudnick, D. R.: Lanthanide Ion Probes of structure in biology. Laser-Induced Luminescence decay constants provide a direct measure of the number of metal coordinated water molecules. *J. Am. Chem. Soc.* **101**, 334 (1979).
25. Randall, S. R., Sherman, D. M., Ragnarsdottir, K. V., Collins, C. R.: The mechanism of cadmium surface complexation on iron oxyhydroxide minerals. *Geochim. Cosmochim. Acta* **63**, 2971 (1999).
26. Spadini, L., Manceau, A., Schindler, P. W., Charlet, L.: Structure and stability of Cd²⁺ surface complexes on ferric oxides. I. Results from EXAFS spectroscopy, *J. Colloid Interface Sci.* **168**, 73 (1994).
27. Rizkala, E. N., Choppin, G. R.: *Handbook on the physics and chemistry of Rare Earths.* (Gschneidner, K. A. J., Eyring, L., Eds.), Elsevier Science, Amsterdam, North-Holland (1991), p. 393.
28. Farley, K. J., Dzombak, D. M., Morell, F. M. M.: A surface precipitation model for the sorption of cations on metal oxides. *J. Colloid Interface Sci.* **106**, 226 (1985).